Improvement on the Efficiency of Condensing Units: Analysis of Cool-n-Save®

Researchers:

Jillian Chodak

Suzanne Murphy

Dr. Robert G. Watts

Tulane University

Department of Mechanical Engineering

New Orleans, Louisiana

May 20, 2005

Improvement on the Efficiency of Condensing Units: Analysis of the CoolNSave™

Jillian Chodak
Suzanne Murphy

Department of Mechanical Engineering, Tulane University, New Orleans, La
May 20, 2005

Abstract

The efficiency of condensing units in air conditioning systems can be improved by spraying water into the air flowing over the condensing coils. A device called the CoolNSave™ was purported to improve the efficiency of a condensing unit by doing just that. Our original hypothesis was that evaporation from the spray would reduce the dry bulb temperature of the air flowing over the condenser. Instead, we found that the effects of evaporative cooling on the air and the evaporation of the water collecting on the fins of the condenser both reduced the temperature of the fins, thereby increasing the heat transfer from the condensing refrigerant.

Introduction

Air-conditioning units use condensers in order to change vaporous refrigerant into liquid on the hot-side of the air-conditioning system. These systems operate by forcing air through the unit while refrigerant enters the unit inside tubing. The air flowing over the tubes absorbs heat from the refrigerant, causing the refrigerant to condense.

The purpose of this study is to determine the effectiveness of a device called The CoolNSave™. This device is purported to increase the efficiency of an air-conditioning unit by releasing a liquid spray into the air that cools the condenser when the condenser is on. Increasing the efficiency of home energy use is clearly important both from a cost standpoint and to reduce energy consumption for environmental reasons.

The CoolNSave™ consists of one inlet hose and three outlet hoses. The inlet hose is connected to a regular garden hose. The three outlet hoses are connected through a mechanism that distributes the water from the garden (inlet) hose to the three outlet hoses only when a lever is raised. The device is affixed to the top of the condenser of a normal air conditioning unit such that when the condenser turns on, the air expelled from the top of the unit raises a lever on the CoolNSave™, which in turn sprays water droplets from three outlet nozzles positioned around the air intake of the condenser.

Our original hypothesis was that the water droplets added to the entering air would reduce the dry bulb air temperature through evaporative cooling. The water droplets are assumed to be uniform spheres, reducing in size through evaporation.

We first measured the velocity of the air entering a condenser using a Kestrel® 2000 Pocket Thermo Wind Meter. The momentum equation for droplets was used to determine the droplet paths for a variety of drop sizes. The coefficient of drag on each droplet is found using Faeth's correlation [1]. Droplet evaporation rates were then

calculated using the correlation of Ranz and Marshall [2] and an energy balance was used to determine the resulting air temperature entering the condenser.

Before performing any analysis regarding drop size, path or evaporation, the CoolNSave™ was assembled and tested. Experimental data such as air velocity and condenser inlet and outlet air temperatures, both with and without the CoolNSave™ was collected. The purpose being to obtain numerical values to provide general orders of magnitude for the values of our variables that would be applicable to a typical air-conditioner condenser. The ambient air temperature and humidity were found on WeatherUnderGround.com and used in the analysis [3].

Instructions provided with the CoolNSave™ indicated that the user should place the nozzles six inches (0.15 m) away from the surface of the condenser unit. The control volume used to calculate the drop paths is based on the average surface face of a condenser unit, which is assumed to be 1 m^2, and the 0.15 m distance between the condenser surface and the nozzle.

We assumed that the drops emanate from a point source that is placed such that that when grouped into three sizes, small, medium and large, the small drops will fall into the middle of the top third of the condenser, the medium drops will strike the middle of the condenser, and the large drops will reach the middle of the lower third of the condenser. According to the manufacturer of the nozzles, the droplets leaving the nozzle are no larger than 50 microns. If this is the case, the droplets would evaporate very quickly and

will never fall enough to reach the bottom of the condenser. We observed that the drops coalesced very close to the outlet of the nozzle and the drops were visible to the naked eye and distinguishable on film from a 400 speed disposable camera. Additional testing occurred to determine the actual range of drop diameter sizes with the use of a high resolution video camera, Easter egg dye, and transparencies. The video camera was used to capture the drop path, while the dye was used to add color to the water so that the droplets would be easier to see and measure once captured on the transparency. While the exact droplet size could not be obtained, it was observed that the diameters of the medium and large drops ranged between 500 and 1000 microns.

We then calculated the drop sizes that would reach the surface of the condenser so that the small drops will fall into the middle of the top third of the condenser, the medium drops will strike the middle of the condenser, and the large drops will reach the middle of the lower third of the condenser. The resulting droplet sizes are 325, 680, and 900 microns in diameter. In order to compare the effectiveness in different climates, analysis was carried out in both twenty and seventy percent ambient air humidity.

The moist air entering the condenser unit decreases in temperature caused by evaporative cooling. The droplets in the air evaporate, increase the relative humidity, and thereby decrease the inlet air temperature. The temperature decrease in the inlet air enhances heat transfer between the refrigerant and the air. Droplets collect on the fins of the air side of the condenser. Evaporation from the resulting film causes in a decrease in the surface temperature. We used a standard methodology for evaporative cooling and evaporation

from surfaces to calculate the cooling rate and design parameters for a typical condenser heat transfer design to estimate the improvement in heat transfer [4].

Methods and Materials

During the experimental testing of the CoolNSave™, values for the air velocity, condenser inlet and outlet temperatures both with and without the CoolNSave™, and the ambient air temperature were collected with the use of the Kestrel® 2000 Pocket Thermo Wind Meter. The data collected provided orders of magnitude that apply to a typical air-conditioner so that we had a basis for performing calculations.

Microsoft Excel was used for the bulk of the calculations. As stated previously the initial diameters for the drops studied are 325, 680 and 900 microns. First the mass flow rate for each drop size is calculated. The flow rate of the spray is known to be 0.062 kilograms per second from the data provided by the manufacturer of the nozzle heads. The mass flow rate for each drop size is assumed to be the same so the mass flow rate for all of the drop sizes is one third of the total mass flow, 0.021 kilograms per second. In order to find the number of drops of each size, the mass flow rate of each drop size, 0.021 kilograms per second, is divided by the mass of its respective drop; this provides the drop flow rate in drops per second.

The positions of the drops are calculated where the drops enter the control volume at a constant rate dependent on their mass fraction. The positions of the drops are dependent

on the Reynolds number, the drag forces, the humidity, and diameter of the drop, which is not constant because the drops are evaporating.

$$m_{drop}(t) = V_{drop}(t) \cdot \rho_{water} \qquad (1)$$

The mass of the drops is calculated (equation 1) by multiplying the volume, V, of the drop times the density, ρ, of water which is 998 kg/m^3. The volume of the drop is not constant and is dependent on the rate of evaporation.

$$\mathrm{Re} = \sqrt{\left[\vec{V}_{x,air} - \vec{V}_{x,drop}\right]^2 + \left[\vec{V}_{y,drop}\right]^2} \cdot \frac{D_{drop}}{\nu_{air}} \qquad (2)$$

The Reynolds number, Re, is calculated using the total relative velocity of the drop (equation 2). $\vec{V}$ is a vector velocity, D is the diameter of the drop and ν is the kinematic viscosity.

$$C_D = \frac{24}{\mathrm{Re}}\left[1 + \frac{\mathrm{Re}^{2/3}}{6}\right] \qquad (3)$$

The drag coefficient, C_D, (equation 3) is a function of the Reynolds number, and is found from the correlation for the standard drag curve [1].

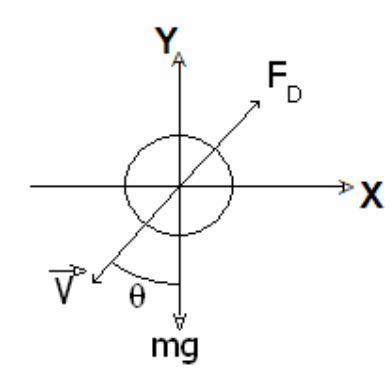

Figure 1 - Droplet schematic which indicates the direction of the drag force, gravitational force, and the resulting velocity vector of the droplet.

The initial angle, θ, of the drops is 90 degrees as measured from the negative vertical axis. The initial drop velocity in both the X and Y directions is zero.

$$\frac{d}{dt}\left(m_d \vec{V}_X\right) = -C_D \cdot \frac{1}{8} \cdot \pi \cdot D^2 \cdot \rho_{air} \cdot \left[\vec{V}_X - \vec{V}_{air,X}\right]\left|\vec{V}_X - \vec{V}_{air,X}\right| \cdot \sin\theta \qquad (4)$$

$$\frac{d}{dt}\left(m_d \vec{V}_Y\right) = -C_D \cdot \frac{1}{8} \cdot \pi \cdot D^2 \cdot \rho_{air} \cdot \left[\vec{V}_Y - \vec{V}_{air,Y}\right]\left|\vec{V}_Y - \vec{V}_{air,Y}\right| \cdot \cos\theta - m_{drop} \cdot g \qquad (5)$$

The acceleration in each direction is calculated using equations (4) and (5) where *g* is the gravity constant.

We used a standard finite difference method to calculate the velocities. The path of the droplets for each size range was then plotted using Microsoft Excel.

The mass of vapor leaving the drops and entering the air is needed both for each drop and for the system so that the change in the relative humidity and the change in the diameter of each drop can be calculated. The change in drop size is included in the solution of the momentum equations.

First the mass of vapor already in the control volume of air is calculated for the relative humidity of both twenty and seventy percent. The Sherwood number (equation 7) is the dimensionless concentration gradient at the surface of the drop. The Sherwood number is calculated using the correlation of Ranz and Marshall. It is a function of the Schimdt number and the Reynolds number [2]. The Schmidt number (equation 6) is the kinematic viscosity divided by the diffusivity of water vapor in air.

$$Sc = \frac{\nu}{D_{AB}} \qquad (6)$$

$$\overline{Sh_D} = 2 + .6\,\mathrm{Re}_D^{1/2} \cdot Sc^{1/3} \qquad (7)$$

$$\overline{h_m} = \frac{\overline{Sh_D} \cdot D_{AB}}{D} \qquad (8)$$

The mass transfer convection coefficient is found from equation (8) where the Sherwood number is multiplied by the diffusivity of the water vapor into the air and divided by the diameter of the drop. Diffusivity was found to be 0.26E-4 m^2/s [5].

$$\dot{n} = \overline{h_m} \cdot A_s \cdot \left[\rho_{A,S} - \rho_{A,\infty}\right] \qquad (9)$$

The rate of evaporation (equation 9) in kilograms per second is calculated from the convection coefficient, the surface area of the drop, the saturation temperature of water at 16°C and the relative humidity.

$$Total\ mass\ of\ vapor\ leaving\ drops = \sum_{s,m,l}\left[\dot{n} \cdot \Delta t \cdot n_{drops}\right] \qquad (10)$$

Then the evaporation rate (equation 10) in kilograms per second is multiplied by the length of the time step. This provides the mass evaporated during the time step and is used in calculating the final mass of the drop for the same time step. The evaporation rate is also used in finding the total amount of water that has evaporated from all of the drops in the control volume.

In order to determine the effect of evaporative cooling due to the evaporation of the droplets, the temperature difference of the intake air with and without the CoolNSave™ is needed. To calculate the dry bulb temperature near the surface of the condenser when the CoolNSave™ is on, the relative humidity after evaporation, φ_f, at the inlet is used.

$$\omega_i = 0.622 \cdot \left[\frac{\varphi_i \cdot P_g(T)}{1.01325 - \varphi_i \cdot P_g(T)} \right] \quad (11)$$

$$\omega_f = \omega_i + \frac{\dot{m}_{vapor}}{\dot{m}_{air}} \quad (12)$$

$$\omega_f = 0.622 \cdot \left[\frac{P_v}{1.01325 - P_v} \right] \quad (13)$$

$$P_g(T) = \frac{P_v}{\varphi_f} \quad (14)$$

In equations (11) through (14) ω_i and ω_f represent the initial and final humidity ratios respectively. P_v is the partial pressure of the vapor and P_g is the saturation pressure at the referenced temperature. The steam tables were used to determine the final dry bulb temperature associated with the P_g(T) value obtained in equation (14) [6].

As drops reach the condenser without fully evaporating, they accumulate on the fins forming a thin film. In this case it becomes important to calculate how much the heat transfer is improved by the evaporation of the water on the fins. First the heat transfer is calculated for the case where there is no water on the fins (equation 18), then the heat transfer is calculated for the case when the water is present (equation 19). In order to carry out this analysis a methodology outlined by Kakaç, S. and Liu, H. is used [4].

The mass flow rates of the air and the refrigerant were calculated. For an air-conditioning unit rated at 10kW the required mass flow rate of the refrigerant is found by dividing the power of the air-conditioning by the enthalpy of vaporization, h_{fg}, for the working fluid and is 0.0605 kg/s [7]. The mass flow rate of the air was calculated next.

The temperature of the air is assumed to increase from 18°C to 26°C, indicating that the mass flow rate of the air is equal to the power of the air-conditioning unit divided by the constant pressure specific heat, $c_{p.a}$, multiplied by the change in air temperature and is 1.24 kg/s [8].

$$G_a = (\rho \mathrm{V})_a \qquad (11)$$

The heat transfer coefficient of the air is a function of the mass flux, G_a (equation 11).

$$\mathrm{Re}_a = \frac{G_a \cdot D_{h,a}}{\mu_a} \qquad (12)$$

Using the geometry of the tube configurations in the condenser, the Reynolds number of the air, Re_a, flowing over the tubes was calculated (equation 12) where $D_{h,a}$ is the hydraulic diameter [9]. The geometric configuration for the tubes in the condenser is 7.75-5/8 T, a fairly typical configuration for an air-conditioner condenser.

Then the air side heat transfer coefficient, h_a, was extrapolated using the Reynolds number from a chart by Kays and London and is found to be 61 W/m^2°C [9].

$$G_l = \frac{\dot{m}_l}{A_l} \qquad (13)$$

$$\mathrm{Re}_l = \frac{G_l \cdot (1-x) \cdot d}{\mu_l} \qquad (14)$$

$$\mathrm{Re}_v = \frac{G_l \cdot x \cdot d}{\mu_v} \qquad (15)$$

The Reynolds number for the liquid portion (equation 14) and the vapor portion (equation 15) of the condensate are calculated. The quality, x, of the condensate is assumed to be 0.5, and the condensate velocity of the refrigerant inside the tube is assumed to be 0.05 m/s [10]. The area of the liquid refrigerant, A_l, is the product of the number of sides (three) the condensate velocity, the frontal area of one tube and the density ratio of vapor refrigerant to liquid refrigerant and is used to calculate the mass flux of the liquid, G_l (equation 13). The liquid mass flux is calculated by dividing the liquid mass flow rate by the area of the liquid refrigerant in the tubes. The Reynolds numbers are functions of the liquid mass flux, G_l, the quality, x, the inner diameter, d, as defined by its configuration, and the viscosities μ_l and μ_g which are the liquid and vapor viscosities of the refrigerant.

$$\mathrm{Re}_{eq} = \mathrm{Re}_v \left(\frac{\mu_v}{\mu_l} \right) \left(\frac{\rho_l}{\rho_v} \right)^{0.5} + \mathrm{Re}_l \qquad (16)$$

Then the equivalent Reynolds number (equation 16) is calculated, where, ρ, is the density, and the subscript, l, is denotes liquid, and the subscript, v, denotes vapor.

$$h_{TP} = 0.05 \cdot \mathrm{Re}_{eq}^{\ 0.8} \cdot \mathrm{Pr}_l \cdot \frac{k_l}{d} \qquad (17)$$

Subsequently the heat transfer coefficient for the refrigerant side is calculated (equation 17), where k_l is the thermal conductivity of the refrigerant. [10]

$$U_a = \left[\frac{A_o}{A_i} \frac{1}{h_i} + A_o R_w + \frac{1}{\eta h_o} \right]^{-1} \qquad (18)$$

Using the previously calculated heat transfer coefficients for the air and the refrigerant, the overall heat transfer coefficient, U_a, is calculated (equation 18). The term A_o

represents the outside heat transfer area of the tube condenser and the term A_i represents the heat transfer area inside the tube condenser. The thermal resistance of the tube wall, R_w, is negligible and η has a value of 0.95 and is the total efficiency of the fin for the given geometric configuration. Once the overall heat transfer coefficient is known, the heat transfer per unit area can be obtained as the product of the overall heat transfer coefficient and the temperature difference between the air and the refrigerant temperatures.

$$q'' = U_a \cdot \Delta T \qquad (19)$$

The heat flux, *q''*, is calculated by multiplying the previously calculated overall heat transfer coefficient by the temperature difference between the refrigerant and the air entering the condenser unit (equation 19). The same equation can be used to determine the temperature of the fins, which is a value between the air and the refrigerant temperatures. The fin temperature determined with this step provides the temperature of the fin without the CoolNSave™.

Next the air inlet temperatures were calculated including the effects of evaporative cooling. By using an iterative method, the decreased temperatures of the inlet air were solved for both the 70% humidity and 20% humidity cases (equation 20).

$$\left(h_{a2} + \omega_2 h_{g2}\right) = \left(h_{a1} + \omega_1 h_{g1}\right) \qquad (20)$$

A heat balance for the system without water evaporating from the fins was next considered (equation 21). The inlet air temperatures determined from the effects of evaporative cooling are used. On the air-side surface, heat is exchanged from the cooled air and the refrigerant, while the liquid water on the surface of the fins is causing cooling

due to evaporation. The temperature on the air side surface is determined by the balance among the heat transfer from the refrigerant, the heat transfer from the outside air, and the evaporation of the water, which cools the surface.

$$\left(T_{refr} - T_{fin}\right) \cdot h_{refr} + h_a \cdot \left(T_a - T_{fin}\right) = h_m \cdot h_{fg,water} \cdot \rho_{sat,water\ vapor} \cdot \left(1 - \phi\right) \qquad (21)$$

This calculation was performed for both the twenty percent and seventy percent humidity cases.

Next the overall heat transfer for the fins is calculated for the case where the air is cooled due to evaporative cooling (equation 22). In this case the fin temperature is fixed, so the heat transfer is no longer dependent on the air temperature. It is only a function of the heat transfer from the refrigerant to the fins.

$$U_a = \left[\frac{A_o}{A_i}\frac{1}{h_i}\right]^{-1} \qquad (22)$$

Equation (19) is then used with the overall heat transfer coefficient determined in equation (22) and the fin temperatures determined from equation (21) to determine the heat flux values associated with the use of the CoolNSave™.

Finally the overall heat transfer is calculated for the combined conditions of inlet air cooled by evaporative cooling and accumulated water evaporating from the fins. The fin temperatures are recalculated (equation 21) with the inlet air temperatures adjusted to the cooled temperatures determined by the effects of evaporative cooling and the revised saturation densities changed by the new temperatures and humidity levels. This was performed for both the initial 70% humidity and 20% humidity cases. After determining

the fin temperatures associated with the combined effects, the new heat flux values are determined between the refrigerant and the fins (equation 19). These heat flux values represent the total improved heat transfer provided by the use of the CoolNSave™ in climates of both high and low humidity.

Results

During the experimental testing of the CoolNSave™ , the inlet air velocity was found to be 2.05 m/s using the Kestrel® 2000 Pocket Thermo Wind Meter. The condenser inlet and outlet air temperatures were also measured. The intake air close to the surface of the condenser remained the same as the ambient air when measured without the CoolNSave™ , but was on average ten degrees (Celsius) cooler than the ambient air with the addition of the CoolNSave™ .

The drop sizes are calculated so that the drops reach the surface of the condenser so that the small drops will fall into the middle of the top third of the condenser, the medium drops will strike the middle of the condenser, and the large drops will reach the middle of the lower third of the condenser. The resulting droplet sizes are 325, 680, and 900 microns in diameter.

Calculations were performed to model the drop paths for each drop size in both twenty and seventy percent humidity. Prior to developing a full model combining the effects of evaporation and drop acceleration, incremental calculations were made to determine various characteristics of the model independent of other factors.

Initiating the progressive calculations towards a full model, the effects of evaporation were calculated on a single stationary drop evaporating in ambient air for the two humidity levels, twenty percent and seventy percent. Droplets reach steady evaporation very quickly [11]. Through the principles of conservation of mass in the control volume, the iterative calculations allowed mass at each time step to evaporate from the droplet and be included into the humidity of the air for the next time step. Similarly, the change in humidity at each time step was reflected in the evaporation rate. Calculations were performed for each drop size.

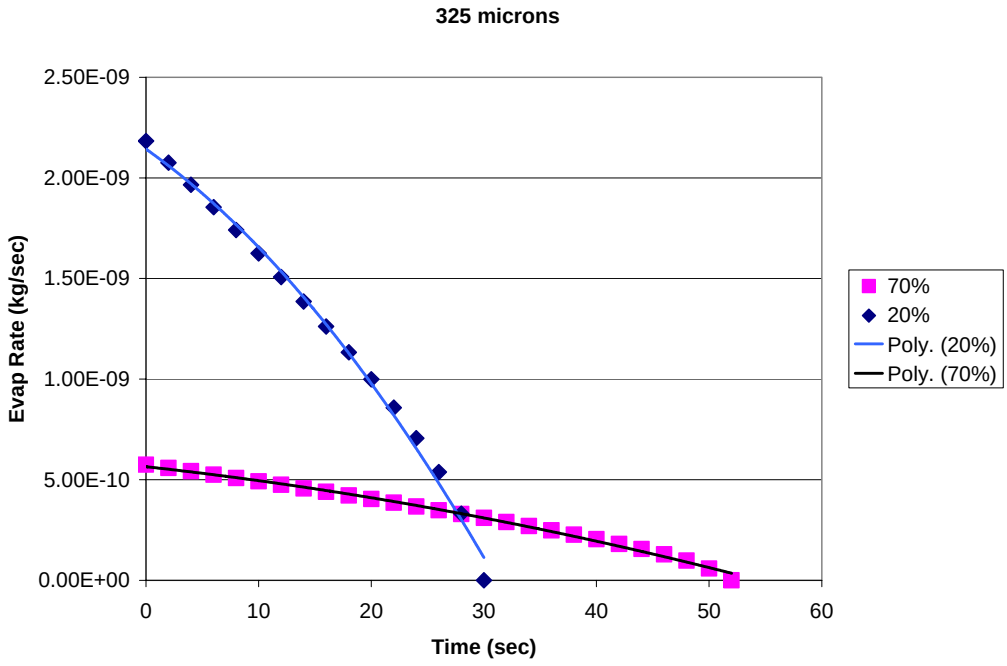

Figure 2 – The evaporation rate for a 325 micron diameter drop in an ambient air control volume, shown here against time, decreases until the drop is completely evaporated.

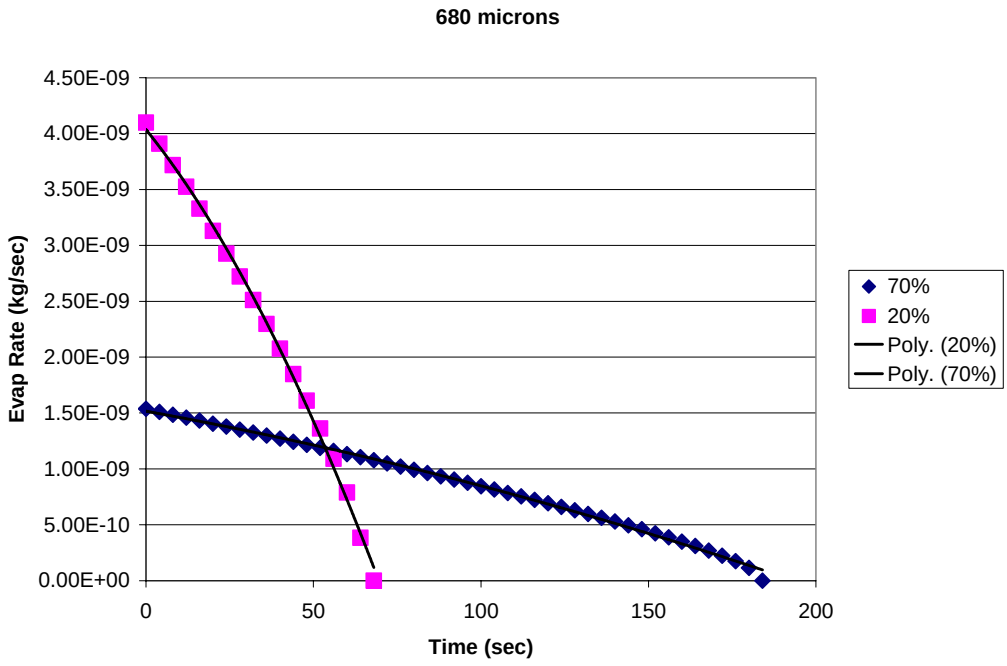

Figure 3 - The evaporation rate for a 680 micron diameter drop decreases similarly to the 325 micron drop. The evaporation rate slows as the drop evaporates until the drop is completely vaporized.

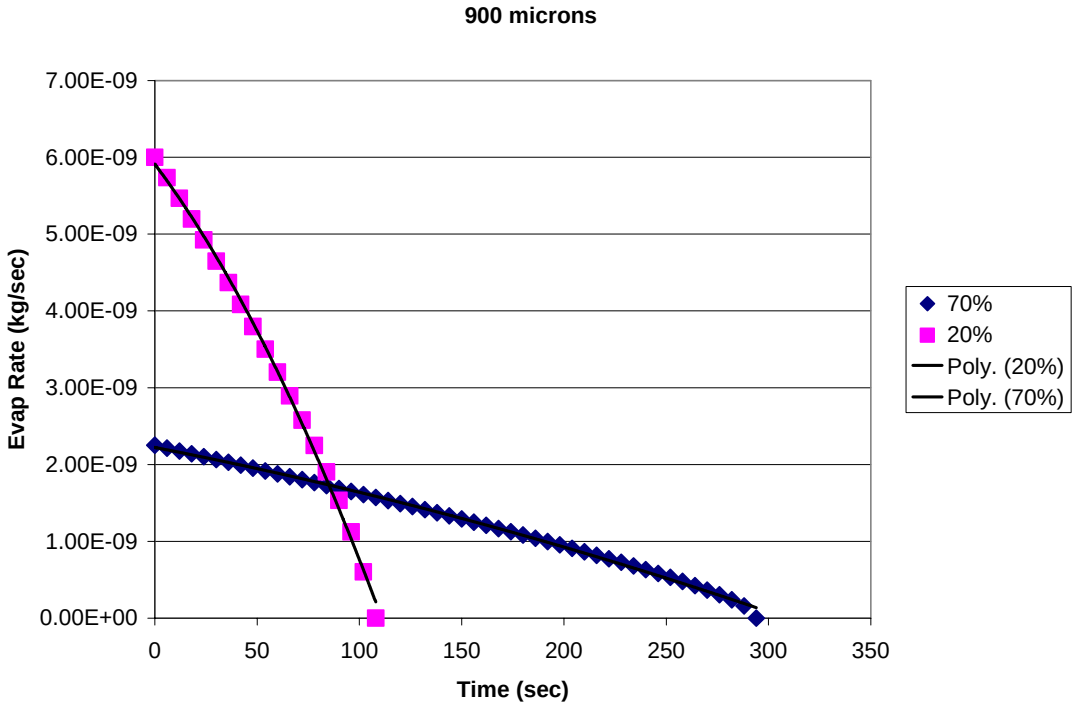

Figure 4 - The evaporation rate for a 900 micron diameter drop also decreases similarly to the other two diameters. The evaporation rate slows as the drop evaporates until the drop is completely vaporized.

It is notable that for all three diameter sizes the evaporation rate decreases more rapidly in the case of twenty percent humidity in ambient air than in seventy percent humidity. Also for all three diameters, complete evaporation of the droplet takes place considerably faster in lower humidity.

Next, the trajectories of a single at each drop size were calculated without including the effects of evaporation. Assumptions included in the calculations were initial velocities equal zero in both the x- and y-directions, the initial x-position was set at six inches away from the surface, and the initial y-position was set at thirty-one inches above the ground, corresponding to the height of the condenser unit used to collect reference data. The iterative calculations performed at each time step reflect the change in relative velocity which in turn affect the Reynolds numbers and drag coefficients. Calculations of this type were performed on all three drop sizes at the two relative humidity levels. The general ambient air humidity, which is set at seventy percent and twenty percent, is considered a constant value in this step of the calculations and is used in the velocity calculations derived from the momentum equations. It should be noted that the drop paths of each drop are slightly different between the two humidity values. The drop passes through the face of the condenser slightly higher in the case of the lower humidity level for all three diameters.

In order to more closely model the CoolNSave™ the effect on a droplet from other droplets is taken into account in the calculations. The drop paths for each drop size were re-calculated to include the effects of the droplets in each respective mass fraction [12].

The evaporation of each drop is expected to slow due to the collective loss of mass from the drops, which in turn elevates the humidity level. The new humidity at each time step was used in calculating the next evaporation rate for the following time step. This is performed at each humidity level and with each drop size. As observed in prior calculations, the drop passes through the face of the condenser at slightly higher elevations in the case of the lower humidity level for all three diameters. It is also notable that the drop diameter for each drop size changed by only approximately 0.5 microns in each case by the time the drops passed through the face of the condenser.

Finally, all of the data was combined to form our most complete working model of the CoolNSave™. All three drops sizes are included in the model; this simulates the full effects of the CoolNSave™ mist. The effects of the evaporation of each drop and the change in the humidity level are also fully modeled. The evaporation effects are calculated and the overall resulting humidity change reflects the cumulative evaporation of all the drops in each time step. The total change in humidity at each time step affects the evaporation of the drops at the next time step. The trajectory of the drops for the twenty percent relative humidity ambient air ranges from 0.02 to 0.09 meters higher than the seventy percent humidity. The model matches our expectations of the actual system.

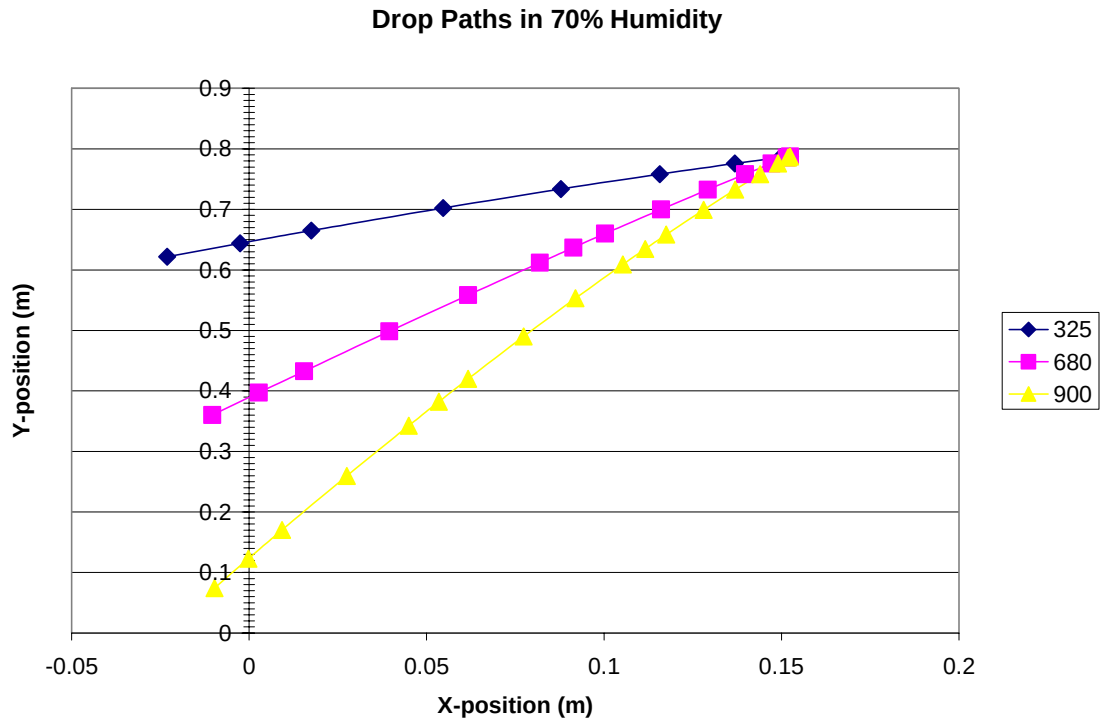

Figure 5 - Paths for drops of each diameter in air of 70% humidity.

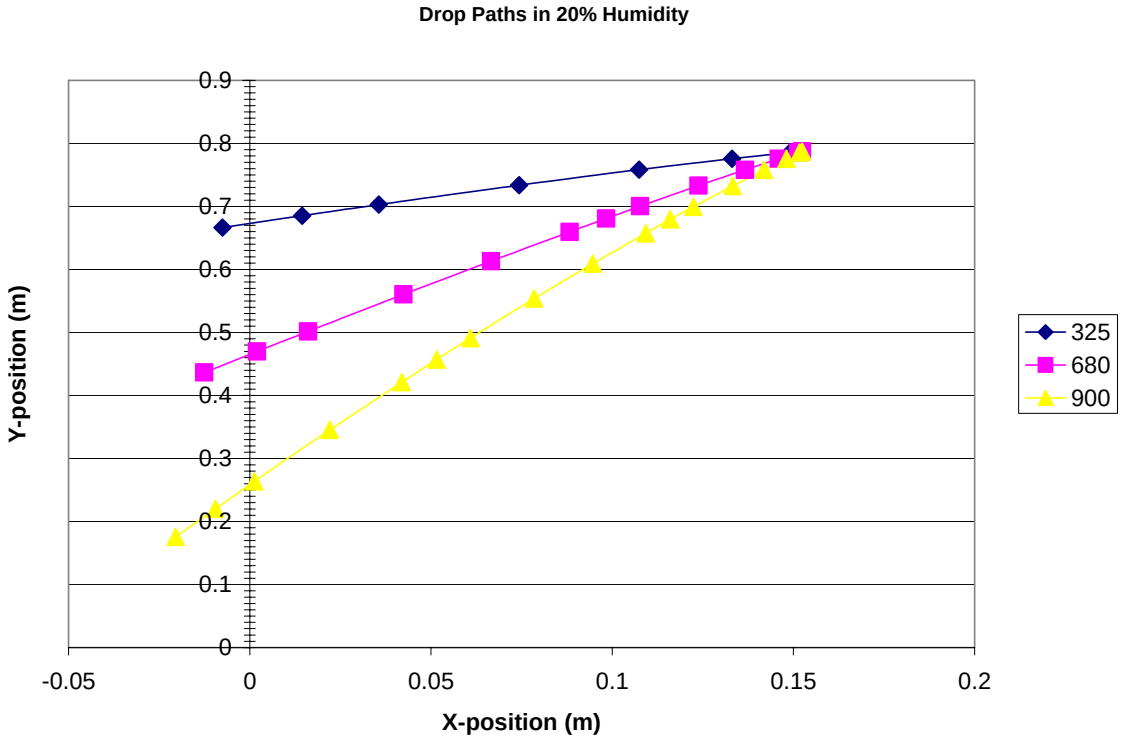

Figure 6 - Paths for drops of each diameter in air of 20% humidity.

Dry bulb temperatures of the air at the condenser surface were calculated using the final humidity calculations obtained from the complete model. Results indicate that the change in air temperature from ambient to the surface of the air-conditioner were minimal. For the case where the initial ambient air humidity was 70% the final humidity was 83%, the final air temperature decreased by 1°K. For the case where the initial ambient air humidity was 20%, the humidity near the surface of the condenser reached 38% and the final temperature of the air decreased by 1.5°K.

In order to draw a comparison for the effectiveness of the CoolNSave™, the heat flux for the tubes in the condenser unit were calculated with and with out the device. First the temperature of the fins on the surface of the tubes was calculated without the use of the CoolNSave™. The model used to determine these values do not include the effects of humidity. The temperature was found to be 301°K and the corresponding heat flux was 400.4 W/m^2. Next the heat flux was determined for the condenser with the evaporative cooling effects of the CoolNSave™ for both the 70% humidity and 20% humidity case. For the 70% humidity case the temperature of the fin was 297.9°K and the corresponding heat flux was 565.9 W/m^2. For the 20% humidity case, the resultant fin temperature was 296.9°K and the heat flux was 616.6 W/m^2. This is considerably higher than the heat flux associated with the unmodified condenser. Finally the heat flux was determined for the condenser with both the evaporative cooling effects and the accumulated water evaporation on the fins due to the CoolNSave™ for both the 70% humidity and 20% humidity case. For the 70% humidity case the temperature of the fin was 294.9°K and the corresponding heat flux was 708.2 W/m^2. For the 20% humidity case, the resultant

fin temperature was 286.9°K and the heat flux was 1080.5 W/m^2. This is considerably higher than the heat flux associated with the unmodified condenser.

	20% Humidity		70% Humidity	
	Heat Flux (W/m^2)	Fin Temperature (°K)	Heat Flux (W/m^2)	Fin Temperature (°K)
Without CoolNSave™	400.4	301	400.4	301
With evaporative cooling effects of CoolNSave™	616.6	296.9	565.9	297.9
With evaporative cooling and accumulated water evaporation effects of CoolNSave™	1080.5	286.9	708.2	294.9

Table 1 – Heat flux and fin temperatures for 20% and 70% humidity without and with the CoolNSave™.

Discussion and Conclusions

The purpose of this study is to determine the effectiveness of the CoolNSave™. Two humidity levels were considered, seventy percent and twenty percent humidity. To accomplish this, the control volume was modeled numerically in a system where humidity is a variable and the drop diameters are variable and reduced by evaporation.

Drop diameters of 325, 680, and 900 microns adhere to the model and are also within the orders of magnitude suggested by our initial experiments. Calculations show that the smallest diameter, 325 microns, passes through the vented surface of the condenser around the centerline of the top third of the condenser face when considering the effects of evaporation. Also, the 680 micron diameter drop passes through the condenser face at the center and the 900 micron diameter drop passes through the face around the centerline of the lower third of the face of the condenser. Drop sizes of the originally suggested

diameter on the order of 50 microns or less would not have fallen far enough in the vertical direction to reach the lower part of the condenser and the drops would also have fully evaporated before reaching the condenser face. Neither of these results reflects what was observed during initial testing.

It is notable that for all three diameter sizes the evaporation rate decreases more rapidly in the case of twenty percent humidity in ambient air than in seventy percent humidity. Also for all three diameters, complete evaporation of the droplet takes place considerably faster in lower humidity. These agree with our expectations about the evaporation of the drop. Both of these observations indicate that the change in air humidity from the ambient to the air humidity at the condenser face should be greater for the 20% humidity case. This behavior is reflected in the complete model. The increase in the humidity level is critical in determining the effectiveness of the CoolNSave™. Because the humidity increase is greater for the 20% humidity ambient air, it was expected that the CoolNSave™ would be more effective in the lower humidity conditions than in the 70% humidity. Our final calculations confirm that this is correct.

Calculations were performed to determine the temperature change of the air due to the evaporative cooling from the drops alone. Using an equation for evaporative cooling, the final temperatures for the air were determined in the 20% and 70% cases. The air temperature for the 70% case was 3.1°K less than the ambient air temperature, providing a 41.3% heat flux increase, and 4.1°K less for the 20% case, providing a 53.9% heat flux

increase. The effects of the evaporative cooling of the air alone substantially increase the heat transfer from the refrigerant.

Concerning the evaporative cooling and accumulated water evaporation calculations, the results indicated that the CoolNSave™ in a 20% humidity climate provides a fin temperature that is 14.1°K lower than the fin temperature determined on an unmodified condenser unit. This corresponds to an increased heat flux of 170% as compared to an unmodified condenser. Even in a high humidity case such as 70% humidity, the fin temperature is lowed by 6.1°K and the heat flux is increased by 76.8%. The implication from these results is that by using a CoolNSave™, even in a climate that endures high humidity, the heat transfer from the refrigerant to the air is substantially increased. This effect implies that cooler air will able to circulate throughout a house and this will decrease the time the condenser unit runs, thus reducing electricity cost to the user.

Acknowledgments

The authors would like to thank Dr. Robert G. Watts for his guidance and support throughout our research.

Figures and Tables

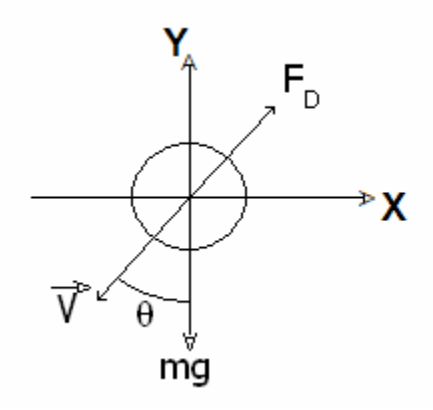

Figure 1 - Droplet schematic which indicates the direction of the drag force, gravitational force, and the resulting velocity vector of the droplet.

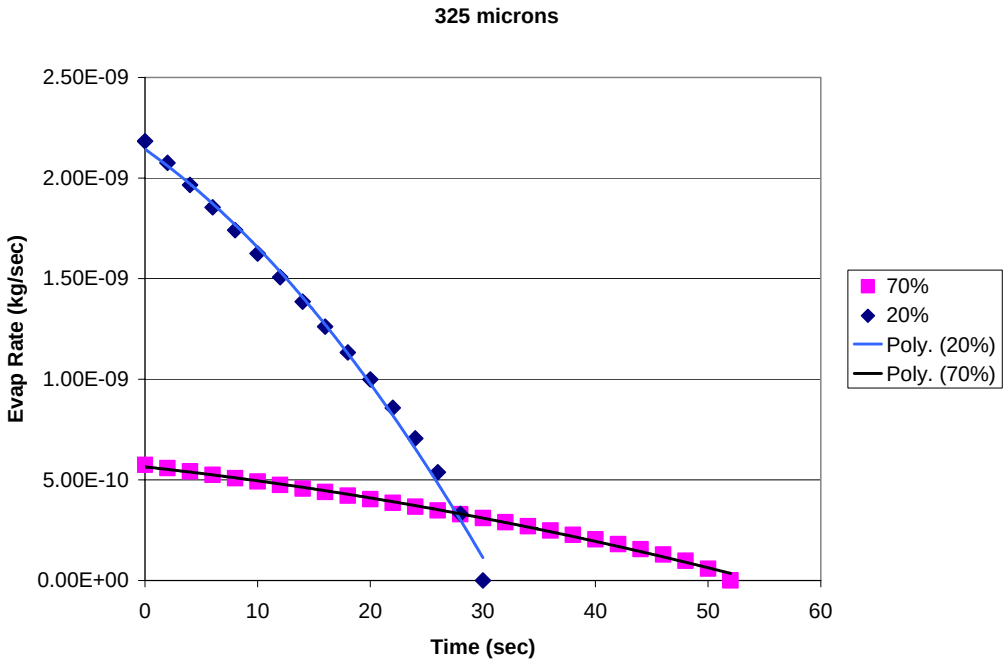

Figure 2 – The evaporation rate for a 325 micron diameter drop in an ambient air control volume, shown here against time, decreases until the drop is completely evaporated.

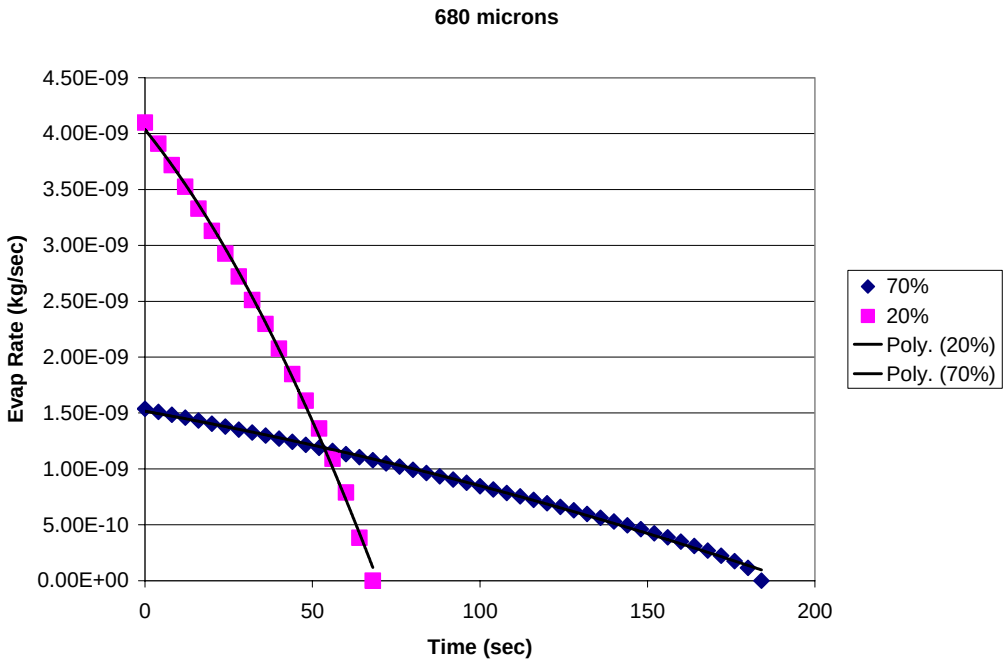

Figure 3 - The evaporation rate for a 680 micron diameter drop decreases similarly to the 325 micron drop. The evaporation rate slows as the drop evaporates until the drop is completely vaporized.

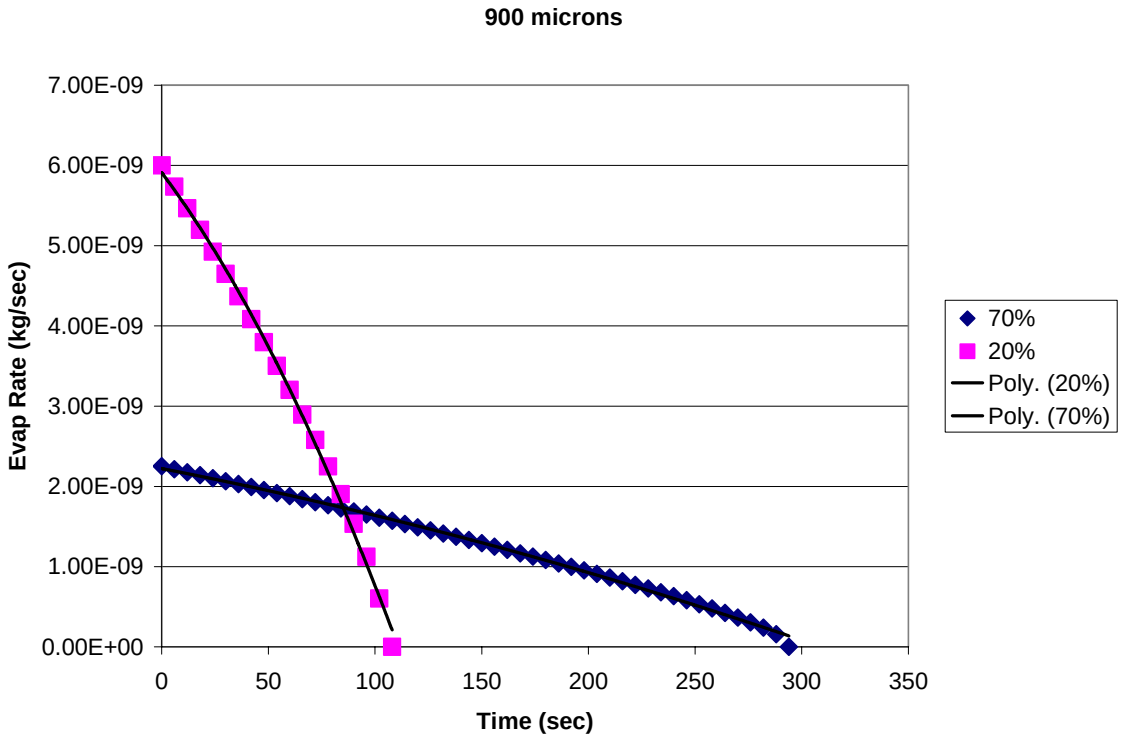

Figure 4 - The evaporation rate for a 900 micron diameter drop also decreases similarly to the other two diameters. The evaporation rate slows as the drop evaporates until the drop is completely vaporized.

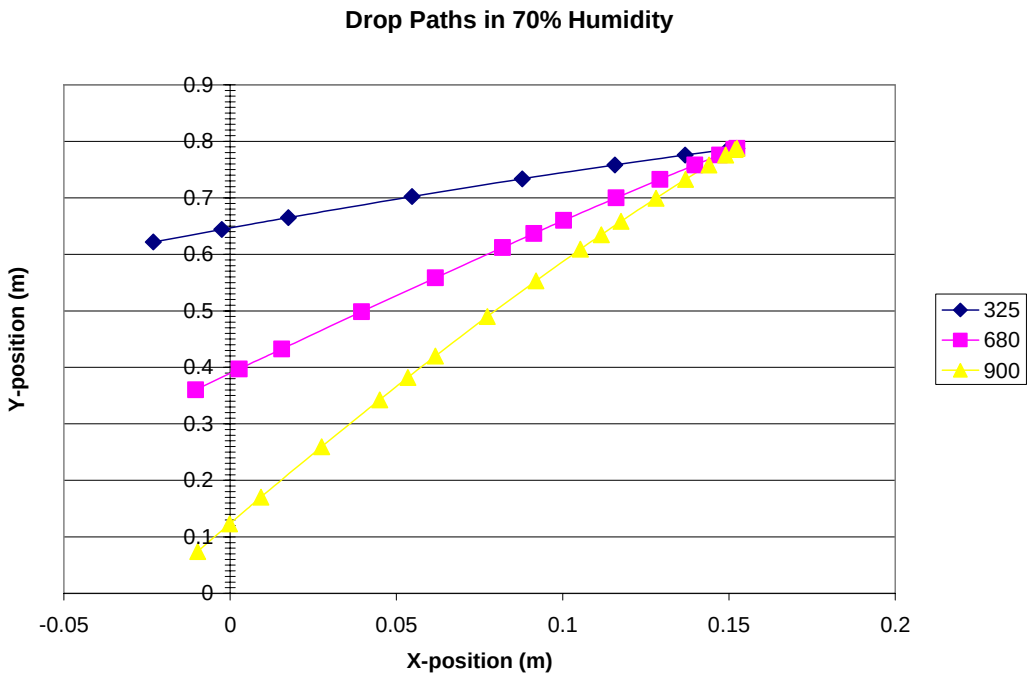

Figure 5 - Paths for drops of each diameter in air of 70% humidity.

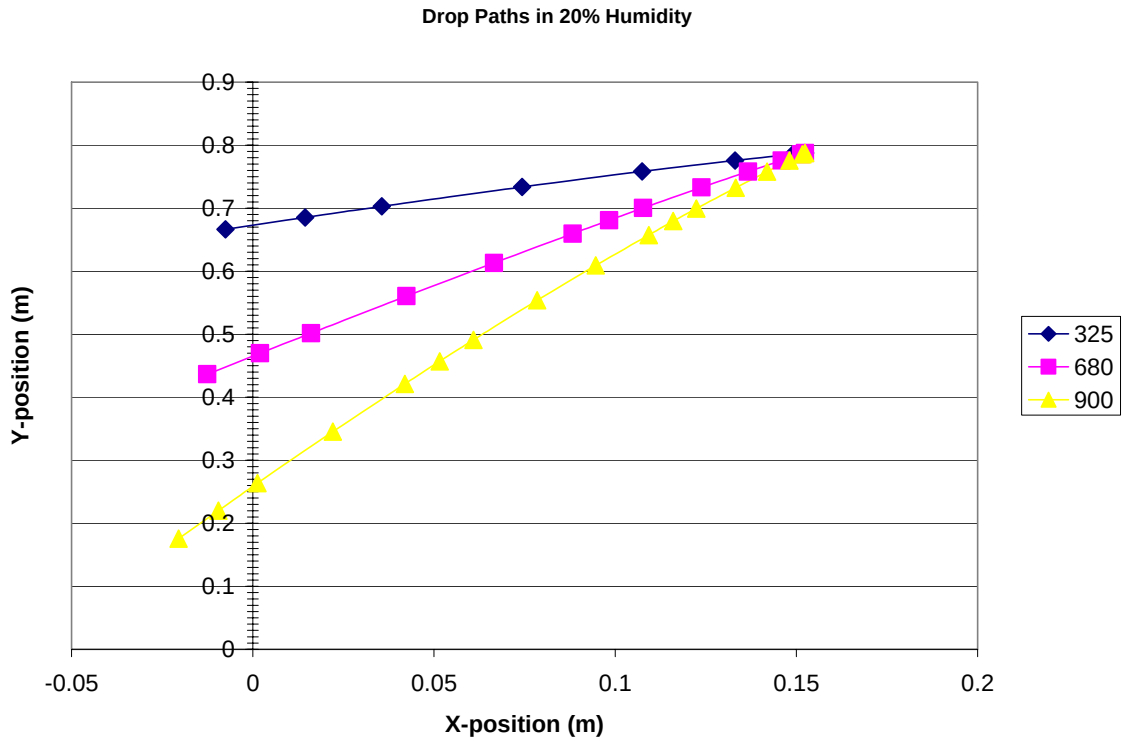

Figure 6 - Paths for drops of each diameter in air of 20% humidity.

	20% Humidity		70% Humidity	
	Heat Flux (W/m^2)	Fin Temperature (°K)	Heat Flux (W/m^2)	Fin Temperature (°K)
Without CoolNSave™	400.4	301	400.4	301
With evaporative cooling effects of CoolNSave™	616.6	296.9	565.9	297.9
With evaporative cooling and accumulated water evaporation effects of CoolNSave™	1080.5	286.9	708.2	294.9

Table 1 – Heat flux and fin temperatures for 20% and 70% humidity without and with the CoolNSave™.

References:

1. Faeth, G.M. (1977) Current status of droplet and liquid combustion, *Prog. Energy Combust. Sci.* 3, 191-224.

2. Ranz, W., and W. Marshall, *Chem. Eng. Prog.,* 141, 1952.

3. "Current Forecast." 2 October 2004. <http://www.weatherunderground.com/cgi-bin/findweather/getForecast?query=new+orleans>.

4. Kakaç, S. and Liu, H., *Heat Exchangers Selection, Rating, and Thermal Design*, 2nd ed., CRC Press, Boca Raton, FL. 2002.

5. Incropera, Frank P. and DeWitt, David P., *Fundamentals of Heat and Mass Transfer, 5th ed.*, John Wiley and Sons, Inc., Hoboken, NJ. 2002.

6. Moran, Michael J. and Shapiro, Howard. N., *Fundamentals of Engineering Thermodynamics, 5th ed.*, John Wiley and Sons, Inc., New York, NY. 2004.

7. Liley, P.E., *Boilers, Evaporators, and Condensers.* Wiley, New York, NY. 1987.

8. Kakaç, S. and Yener, Y., *Convective Heat Transfer*, 2nd ed., CRC Press, Boca Raton, FL. 1985.

9. Kays, W. M. and A. L. London, Compact Heat Exchangers, 3rd ed., McGraw-Hill, New York, 1985.

10. Cavallini, A. and R. Zecchin, A Dimensionless Equation for Heat Transfer in Forced Convection Condensation, Proc. 5th Int. Heat Transfer Conf., 309-313. Sept. 5-7, 1974.

11. Watts, R. (1972) The Maximum Relaxation Times for Evaporating Liquid Droplets. Journal of Atmospheric Sciences Vol. 29, No 1, 208-211.

12. Watts, R. (1971) Relaxation Time and Steady State Evaporation Rate of Freely Falling Raindrops. Journal of Atmospheric Sciences Vol. 28, No 2, 219-225.

13. Abramzon, B. and W. A. Sirignano (1989) Droplet vaporization model for spray combustion calculations. Int. H. Heat Mass Transfer Vol. 32, No 9, 1605-1618.

14. Watts, R. and A. Terry Bahill., *Keep Your Eye on the Ball: The Science and Folklore of Baseball, 2nd ed.*, W.H. Freeman; Pub. Co. 2000.